SUPPORTING INFORMATION

Synthesis, Characterization and Optimization for in Vivo Delivery of a Non-Selective Isopeptidase Inhibitor as New Anti-Neoplastic Agent

Ulma Cersosimo,[†] Andrea Sgorbissa,[‡] Carmen Foti,[‡] Sara Drioli,[†] Rosario Angelica,[‡] Andrea Tomasella,[‡] Raffaella Picco,[‡] Marta Stefania Semrau,[§] Paola Storici,[§] Fabio Benedetti,[†] Federico Berti,[†] Claudio Brancolini,[*‡]*

[†]Dipartimento di Scienze Chimiche e Farmaceutiche, Università degli Studi di Trieste. Via Giorgieri 1 – 34127 Trieste ITALY.

[‡]Dipartimento di Scienze Mediche e Biologiche Università degli Studi di Udine. P.le Kolbe 4 - 33100 Udine ITALY.

[§]Structural biology laboratory, Elettra - Sincrotrone Trieste S.C.p.A., Area Science Park, Basovizza, 34149 Trieste, Italy

Contents

1.	Supplementary figures	S2
2.	Animal studies	S5
3.	Microarray data processing and analysis	S5
4.	Molecular modeling	S5
5.	Synthesis and characterization of compounds **1a**, **2a**, **2b**, **2e**	S7
6.	References	S8
7.	HPLC analysis of biologically tested compounds	S9

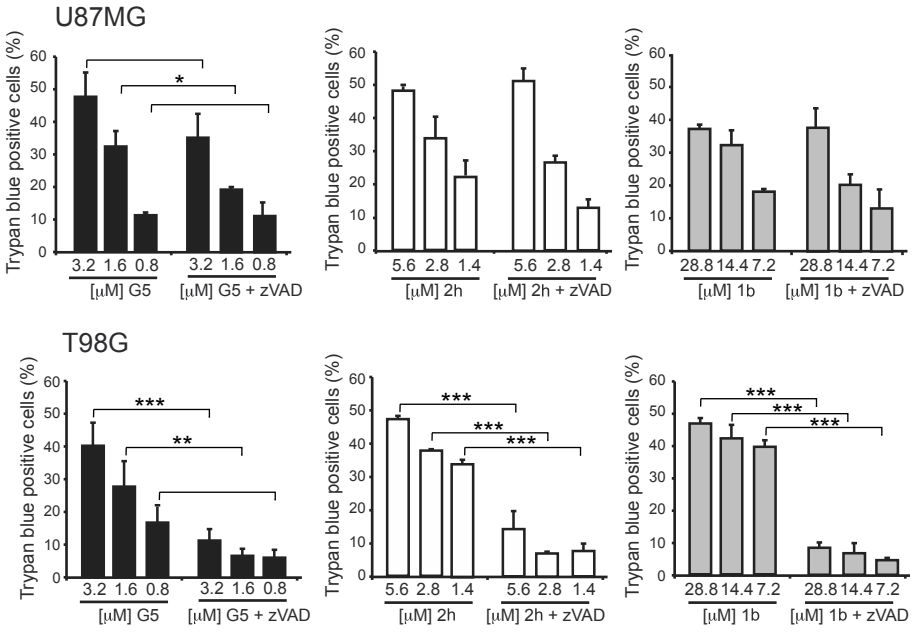

Figure S1. Effect of caspase inhibitor zVAD−fmk cell death (percent of Trypan blue-positive cells) in U87MG (top) and T98G (bottom) cells treated with (left to right): G5, **2h**, **1b**. Columns, mean (n = 3); bars, SD.

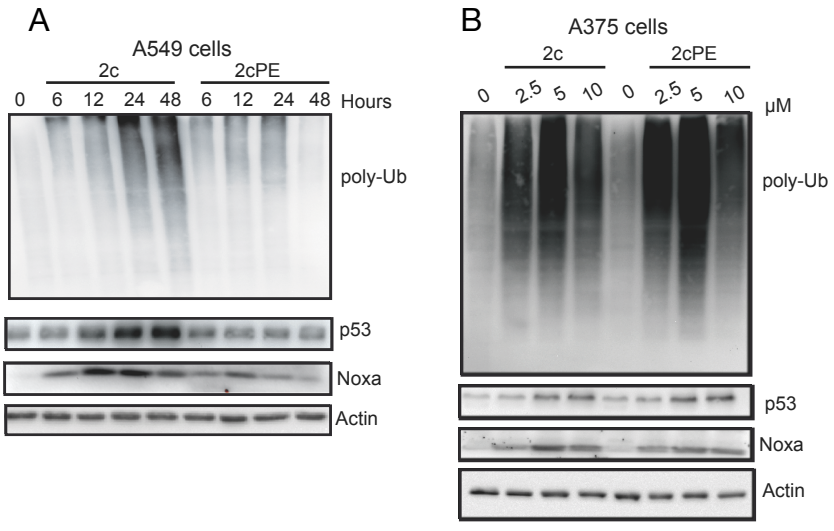

Figure S2. A) Immunoblot analysis showing poly-ubiquitin accumulation, p53 stabilization and Noxa induction in A549 cells treated with 10 μM **2c** and 2cPE (**11**) for 6-48 hours. B) Poly-ubiquitin accumulation, p53 stabilization and Noxa induction in A375 cells treated with 2.5-10 μM **2c** and **11** for 24 hours.

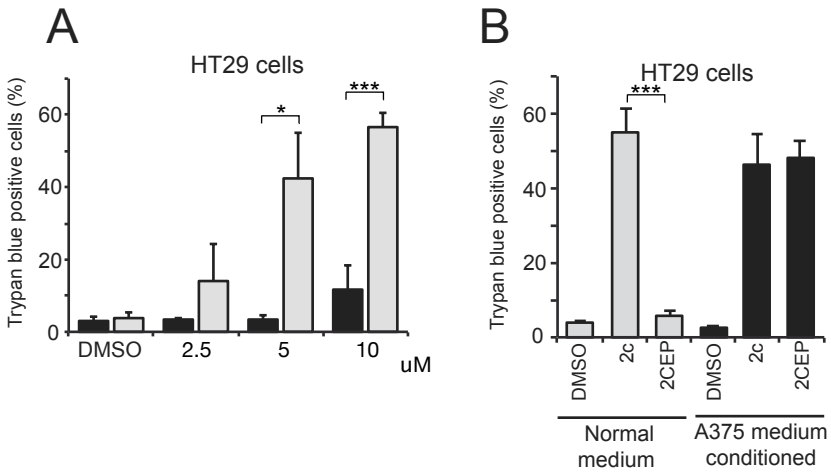

Figure S3. Responsiveness of HT29 cells to 2c and 2cPE treatments.
A) HT29 cells were treated with the indicated concentrations of **2c** (grey columns) and 2cPE (**11**) (black columns) for 48 h. Appearance of cell death was scored by trypan blue staining. Columns, mean (n = 3); bars, SD.
B) HT29 cells were treated with 10μM **2c** and 2cPE (**11**) for 48 h in a normal medium and in a conditioned medium from A375 cell cultures. Appearance of cell death was scored by trypan blue staining. Columns, mean (n = 3); bars, SD.

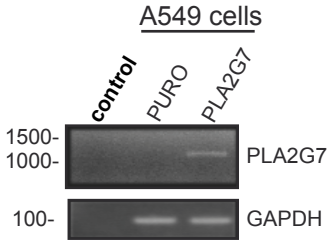

Figure S4. RT-PCR analysis to verify the expression of recombinant PLA2G7 in A549 cells. RNAs were extracted, retro-transcribed and PLA2G7 ORF amplified using Taq polymerase and the corresponding oligonucleotides. GAPDH was amplified as control. In the control PCR was performed in the absence of RNA.

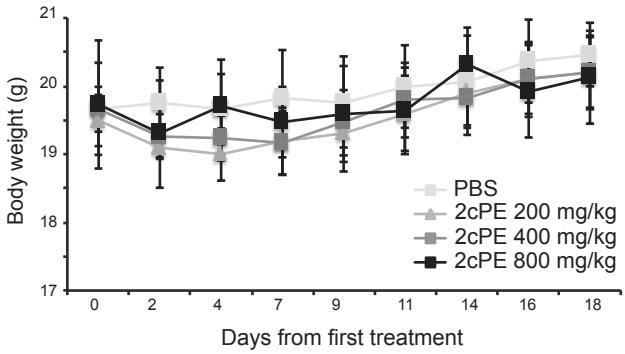

Figure S5. Body weight variations of mice treated with 200-800 mg/kg 2cPE, showing no gross toxicity after 18 days.

Animal studies

Three to four animals were housed in each cage. The animals were kept in a controlled environment, with a light/dark cycle of 12 hours (h) each. Sterile tap water and sterile food was provided ad libitum. All animals were subjected to the same environmental conditions.

Microarray data processing and analysis

CDFs were downloaded from the Molecular and Behavioral Neuroscience Institute Microarray Lab (URL:http:// brainarray.mbni.med.umich.edu/ Brainarray/ Database/ CustomCDF/genomic_curated_CDF.asp). All annotation information were downloaded from the same website. The normalization step was done with the standard MAS5.0 algorithm, described in the Statistical Algorithms Description Document available from Affymetrix (URL: http:// www.affymetrix.com/ support/ technical/ whitepapers/ sadd_whitepaper.pdf).

Modeling of the PLA2G7 catalyzed hydrolysis of PEGylated 2c. The model was built from the crystal structure of PLA2G7 covalently inhibited by paraoxon (PDB: 3D5E) following the logical scheme shown in Figure S5.

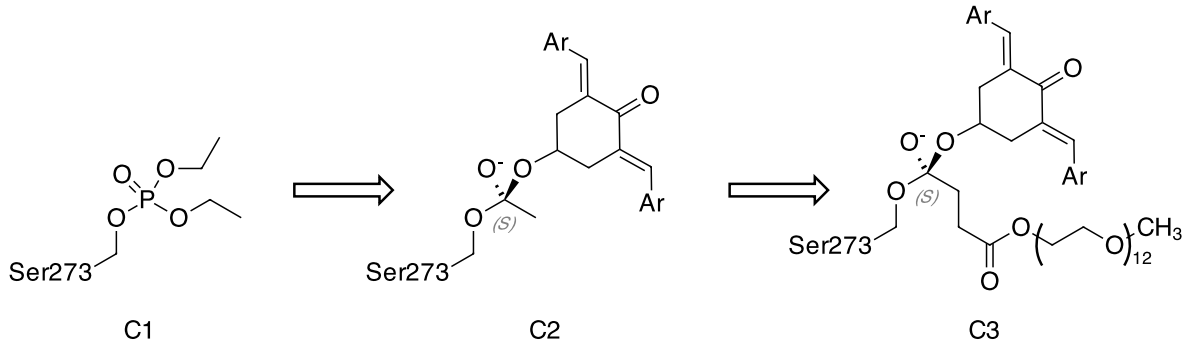

Figure S6. Logical scheme for the construction of a model of the tetrahedral intermediate for the phospholipase 2A catalysed hydrolysis of 2cPE

Starting the 3D5E crystal structure, initially all the hydrogen atoms were added assuming a pH environment of 7.5, then all the crystallization water molecules were removed, and this reference complex (C1, Figure S5) was allowed to relax. The initial geometry of the enzyme tetrahedral intermediate was built by docking a simplified substrate (acetylated **2c**) onto the structure of the phosphonate portion of the optimized reference complex C1. Both possible configurations at the reactive carbon were considered, and the conformational space accessible to the tetrahedral intermediates was explored. A set of sterically tolerable conformations was generated by a systematic search carried out on all the rotatable bonds of the serine-bound intermediates, and only the *S* intermediate C2 gave low energy relaxed structures. The unique conformation corresponding to a productive intermediate was then selected by structural analysis: the stereoelectronic theory of Deslongchamps predicts that in a tetrahedral intermediate for ester hydrolysis, the C–O bond can be cleaved efficiently only if both the remaining oxygens of the intermediate have a lone pair orbital antiperiplanar to the breaking bond (Figure S6).[1]

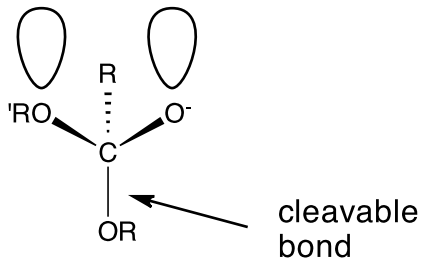

Figure S7. Productive conformation of the intermediate for ester hydrolysis

This condition has proven to be effective in explaining the selectivity of lipase catalyzed reactions[2] and it is satisfied only if the geometry around the O(Ser273)–C–O–R dihedral angle is *anti*, as in C2. In our case this conformation may be obtained in a unique way without the occurrence of unfavourable contacts. It also allows establishing the optimal hydrogen bond network between the oxyanion hole residues and the intermediate, which was then optimized starting from this geometry. After this first stage, a succinate moiety esterified with a polyethylene glycol dodecamer was added in order to mimic 2cPE. The chain was easily placed inside the channel leading to the hydrophobic interface, and the whole structure C2 thus obtained was finally optimized.

Synthesis and characterization of compounds 1a, 2a, 2b, 2e.

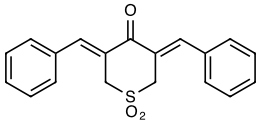

(*3Z,5Z*)-3,5-Bis(benzylidene)-tetrahydro-4*H*-thiopyran-4-one-1,1-dioxide (1a). 21% from tetrahydro-4*H*-thiopyran-4-one-1,1-dioxide and benzaldehyde, following the literature procedure;[3] m.p. 195–198 °C (lit.[3] 198–200 °C). ^{1}H NMR: δ = 4.44 (s, 4H), 7.45 (m, 10H), 8.0 ppm (s, 2H). ^{13}C NMR: δ = 53.2, 126.8, 129.1, 129.7, 130.1, 133.6, 144.3, 186.3 ppm. IR: ν = 1664 (SO_2), 1325 and 1128 cm^{-1} (SO_2). MS: *m/z* 324 (M^+ 30%), 259 (100%).

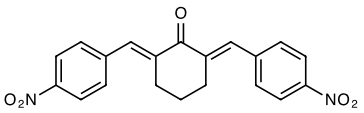

(*2E,6E*)-2,6-Bis[(4-nitrophenyl)methylene]cyclohexanone (2a). 70% from cyclohexanone and 4-nitrobenzaldehyde, following the literature procedure;[4] m.p. 200–203 °C. ^{1}H NMR: δ = 1.84 (m, 2H), 2.92 (m, 4H), 7.58 (d, 4H), 7.79 (s, 2H), 8.26 ppm (d, 4H). ^{13}C NMR: δ = 22.6, 28.4, 123.8, 130.8, 134.9, 138.7, 142.2, 147.4, 189.3 ppm. IR: ν = 1670 (C=O), 1513 and 1342 cm^{-1} (NO_2). MS: *m/z* 364 (M^+ 10%).

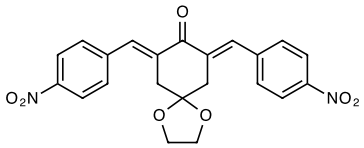

***(7E,9E)*-7,9-Bis[(4-nitrophenyl)methylene]-1,4-dioxaspiro[4,5]decan-8-one (2b).** 52% from 1,4-dioxaspiro[4,5]decan-8-one and 4-nitrobenzaldehyde, following the literature procedure;[4] m.p. 243 °C (from ethanol) (lit.[4] 244–246 °C). ^{1}H NMR: δ = 3.0 (s, 4H), 3.85 (m, 4H), 7.58 (d, 4H), 7.8 (s, 2H), 8.25 ppm (d, 4H). ^{13}C NMR: δ = 37.8, 65.1, 106.0, 123.6, 130.8, 135.4, 136.4, 141.8, 147.0, 187.0 ppm. IR: ν = 1676 (C=O), 1519 and 1342 cm^{-1} (NO_2). MS: *m/z* 422 (M^+ 100%).

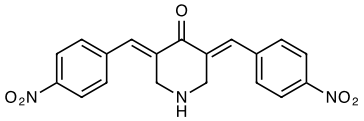

(*3E,5E*)-3,5-Bis[(4-nitrophenyl)methylene]-4-piperidone (2e). 45% from 4-piperidone hydrochloride monohydrate and 4-nitro-benzaldehyde, following the literature procedure;[5] m.p. 233–235 °C (lit.[5] 230–233 °C). ^{1}H NMR ([D_6]DMSO): δ = 4.0 (s, 4H), 7.65 (s, 2H), 7.76 (d, 4H), 8.27 ppm (d, 4H). ^{13}C NMR ([D_6]DMSO): δ = 47.96, 124.14, 131.90, 132.13, 139.58, 142,00 147.66, 198.38 ppm. IR: ν = 3310 (NH), 1661 (C=O), 1520 and 1352 cm^{-1} (NO_2). ESI-MS: 388 (MNa^+), 366 (MH^+).

References

(1) Deslongchamps, P. *Stereoelectronic effects in organic chemistry*; Pergamon Press: Oxford, 1984; pp 54–100.

(2) Berti, F.; Forzato, C.; Nitti, P.; Pitacco, G.; Valentin, E. A study of the enantiopreference of lipase PS (Pseudomonas cepacia) towards diastereomeric dihydro-5-alkyl-4-hydroxymethyl-2(3H)-furanones. *Tetrahedron: Asymmetry* **2005**, *16*, 1091–1102.

(3) Puar, M. S.; Rovnyak, G. C.; Cohen, A. I.; Toeplitz, B.; Gougoutas, J. Z. Orientation of the sulfoxide bond as a stereochemical probe. Thiopyrano[4,3-c]pyrazoles. *J. Org.Chem.* **1979**, *44*, 2513–2518.

(4) Dimmock, J. R.; Padmanilayam, M. P.; Zello, G. a; Nienaber, K. H.; Allen, T. M.; Santos, C. L.; De Clercq, E.; Balzarini, J.; Manavathu, E. K.; Stables, J. P. Cytotoxic analogues of 2,6-bis(arylidene)cyclohexanones. *Eur. J. Med. Chem.* **2003**, *38*, 169–177.

(5) Dimmock, J. R.; Padmanilayam, M. P.; Puthucode, R. N.; Nazarali, A. J.; Motaganahalli, N. L.; Zello, G. A.; Quail, J. W.; Oloo, E. O.; Kraatz, H. B.; Prisciak, J. S.; Allen, T. M.; Santos, C. L.; Balzarini, J.; De Clercq, E.; Manavathu, E. K. A Conformational and Structure-Activity Relationship Study of Cytotoxic 3,5-Bis(arylidene)-4-piperidones and Related N-Acryloyl Analogues. *J. Med. Chem.* **2001**, *44*, 586–593.

HPLC analysis of tested compounds.

All the compounds were analysed on a Phenomenex Luna C18 5μ 150x4.6 mm column. The composition of the mobile phase is reported in table S1 with the retention times and the % area of the main peak. The flow was always 1 ml/min. 20 μl of a 100 μM solution of the compound in acetonitrile were loaded on the column. An UV detector set at 230 nm was used.

Table S1. Mobile phase, retention time and purity of tested compounds.

Compound	Water	Acetonitrile	Rt/min	%
1a	60	40	15.91	99.9
1b	60	40	58.25	99.7
1c	45	55	2.46	96.2
1d	45	55	7.38	98.5
1e	45	55	11.81	98.2
1f	35	65	4.54	97.1
1g	35	65	3.39	97.7
1h	35	65	5.52	98.3
1i	35	65	3.84	97.9
1j	35	65	5.90	97.7
1k	35	65	9.40	97.7
1l	35	65	6.91	96.8
G5	50	50	10.78	99.1
2a	35	65	10.74	99.2
2b	60	40	30.92	98.8
2c	55	45	11.79	98.8
2d	55	45	40.23	95.7
2f	50	50	22.97	98.4
2g	50	50	37.19	96.7
2h	50	50	6.19	97.3